

TK-2361

NACA TN 2361

TECHNICAL LIBRARY
AIRESEARCH MANUFACTURING CO.
9851-9951 SEPULVEDA BLVD.

INGLEWOOD,
CALIFORNIA

NATIONAL ADVISORY COMMITTEE FOR AERONAUTICS

TECHNICAL NOTE 2361

TURBULENCE-INTENSITY MEASUREMENTS IN A JET OF AIR ISSUING FROM A LONG TUBE

By Barney H. Little, Jr., and Stafford W. Wilbur

Langley Aeronautical Laboratory
Langley Field, Va.



Washington
May 1951

1

NATIONAL ADVISORY COMMITTEE FOR AERONAUTICS

TECHNICAL NOTE 2361

TURBULENCE-INTENSITY MEASUREMENTS IN A JET OF
AIR ISSUING FROM A LONG TUBE

By Barney H. Little, Jr., and Stafford W. Wilbur

SUMMARY

Data are presented for turbulent-velocity-fluctuation components and mean-velocity distributions measured in the subsonic jet issuing from a pipe in which fully developed turbulent flow was established. Boundary conditions were set by mounting this pipe concentrically with a larger pipe and maintaining the maximum velocity in the resulting annulus equal to the mean velocity in the inner pipe.

Axial and radial components of the fluctuation velocities were examined as functions of Reynolds number and position in the jet. The dimensionless velocity profiles varied only slightly with varying Reynolds number. The ratios of the root-mean-square axial turbulent fluctuation velocities to the local mean velocities showed a slight increase with increasing Reynolds numbers. The radial components of the fluctuation-velocity parameter showed no systematic variation with Reynolds number.

The turbulence was not isotropic in the jet formed by the inner pipe. The axial-fluctuation-velocity component was approximately 2.5 times as great as the radial component at the pipe center line. Near the pipe wall at the exit survey station, the axial-fluctuation-velocity component was about 3 or 4 times as great as the radial component.

The axial components of the turbulent fluctuation velocities diminish rapidly downstream of the pipe wall, whereas the radial components are practically constant, so that the axial and radial components approach a condition of equal magnitude with increasing distance from the pipe exit.

INTRODUCTION

An investigation of the flame-propagation properties in burners by the Bureau of Mines of the United States Department of Interior has indicated that, for the correlation of the flame-propagation velocities

with local turbulence intensity in the flow, quantitative turbulence data are needed. In order to obtain such data, an experimental investigation has been made at the Langley Aeronautical Laboratory of the National Advisory Committee for Aeronautics for a configuration closely resembling that of the Bureau of Mines.

The Bureau of Mines configuration is that of a subsonic air jet issuing from a pipe in which fully developed turbulent flow is established. In order to minimize mixing at the jet boundaries, which would hinder the taking of data by optical methods, the burner pipe was centered inside the larger pipe and the air velocity in the resulting annulus was maintained equal to the mean velocity in the inner pipe.

For the investigation reported herein, a 2-inch inside-diameter pipe 65 diameters long was used. This pipe was centered inside another pipe with an inside diameter of 9.5 inches. Near the pipe exit the outer pipe was converged to a 6-inch diameter in order to produce a thin boundary layer on the outer surface of the inner pipe. Every effort was made in designing this apparatus to duplicate the original configuration at the Bureau of Mines as closely as possible.

Data were measured for the axial and radial components of turbulence intensity in the region extending from the pipe exit to a distance 5 diameters out and bounded by the approximate outer edges of the wake formed by the inner pipe wall. Reynolds number (based on pipe diameter) was varied from 20,000 to 120,000. These Reynolds numbers correspond to a velocity range from about 15 feet per second to 115 feet per second. All turbulence measurements were made by the hot-wire anemometer methods described in reference 1.

SYMBOLS

u'	root-mean-square fluctuation velocity in axial direction
v'	root-mean-square fluctuation velocity in radial direction
u	local mean velocity
U	maximum mean velocity along a diameter at any survey station
U_0	maximum mean velocity along a diameter at pipe-exit survey station
r	radial distance from pipe center line; positive and negative signs are used to distinguish between diametrically opposite points at same distance from center line

y	distance along a diameter from pipe wall toward pipe center line
x	axial distance from pipe exit
D	diameter of inner pipe
R	Reynolds number ($U_o D / \nu$)
ν	kinematic viscosity
δ	value of y at point where $u = U$
v_*	shearing stress velocity
n	arbitrary constant in exponential velocity-distribution law

APPARATUS AND METHODS

The experimental apparatus, as shown in figure 1, consists of a 2-inch inside-diameter brass tube concentrically mounted within a 9.5-inch inside-diameter steel pipe. The inner pipe is 130 inches in length with a bell at the inlet and a tapered outer edge at the exit. The outer pipe has an inlet bell of variable area ratio and a converging nozzle with an approximate area ratio of 2.7 to 1 at the exit. The inner surface of the inner pipe was reamed and polished to 2.000 inches in diameter, whereas the pipe surfaces bounding the annulus were smooth machined. The inlet area of both pipes was surrounded with a protective screening for the removal of dust particles and was located in a settling chamber. This settling chamber consisted of a 7- by 7-foot trench closed at one end and having a variable-bleed wall at the other end to provide for the exhaust of excess air.

The hot-wire survey mechanism (fig. 2) was so constructed as to be movable longitudinally with 20 inches of travel from the pipe exit and movable radially to survey across the width of the outer-pipe exit along a diameter. This radial motion could be controlled to 0.001 of an inch. The hot-wire carriage carried, in addition to the hot wire, a 0.040 outside-diameter total-pressure tube used for determining the local mean velocities. A 20-percent iridium 80-percent platinum wire with nominal diameter of 0.00015 inch and approximately 1/8 inch in length, which was prepared by the Wollaston process, was used for all hot-wire measurements. Electrical equipment was constructed by the Langley Instrument Research Division to resemble closely that used by Schubauer and Klebanoff in reference 1. This reference estimates that, for turbulence of the magnitude reported herein, the expected error in measured fluctuation velocities will be less than 5 percent.

The data were taken by moving the hot-wire head diametrically across the jet in small increments and recording the necessary quantities at each point. The total-pressure tube was then moved along the same path to measure pressure at each point. Static pressure was assumed equal to room pressure. From these pressure measurements the local mean velocity was determined. This process was carried out at one distance from the pipe exit for four different Reynolds numbers, starting with the lowest and going to the highest. The survey mechanism was then moved to the next position and the process repeated. At each different Reynolds number it was necessary to set the variable-area inlet bell leading to the annular region in order to maintain the condition that the maximum velocity in the annulus be equal to the mean velocity in the inner pipe.

RESULTS AND DISCUSSION

The turbulent fluctuation velocities u' and v' measured at three axial positions for the range of Reynolds numbers of the tests are presented in table I. Mean-velocity distributions at the pipe exit are plotted in figure 3 for four different Reynolds numbers. The data fit well the exponential distribution law $\frac{u}{U} = \left(\frac{y}{\delta}\right)^{1/n}$, when n is assigned values ranging from approximately 6.7 at $R = 21,300$ up to approximately 8.0 at $R = 115,000$. The agreement of these velocity distributions with the universal distribution law

$$\frac{u}{v_*} = 5.75 \log_{10}\left(\frac{v_* y}{v}\right) + 5.5$$

(reference 2) is shown in figure 4. Since no measurements of wall shearing stress were made, the shearing stress velocity v_* was computed from the empirical formula, $v_* = 0.1823 \left(\frac{2v}{D}\right)^{1/8} \bar{u}^{7/8}$ (reference 2), where \bar{u} is the mean velocity across the pipe.

In figure 5, mean-velocity and turbulence-intensity parameters are plotted against radial distance from the center line r for four different Reynolds numbers R and three values of distance from the pipe exit x/D . In this figure the parameters used are: the ratio of the local mean velocity to the maximum mean velocity along the diameter u/U , the ratio of the root-mean-square turbulent fluctuation velocity in the axial direction to the local mean velocity u'/u , and the ratio of the root-mean-square fluctuation velocity in the radial direction to the local mean velocity v'/u .

From the curves of u'/u and v'/u in figure 5, it can be seen that the turbulence in the inner pipe jet is not isotropic. In the region near the pipe center line u'/u is about 2.5 times as great

as v'/u . Near the pipe wall u'/u is about 3 or 4 times greater than v'/u . Both quantities are distributed in a similar manner with their maximum values close to the wall.

Evidence of some asymmetry is noted in these distributions - very slight at the lower Reynolds numbers but more pronounced as Reynolds number increases. At the higher Reynolds numbers the peaks of the distribution curves lie at about $r = -0.1$ inch. Since this displacement does not increase at positions farther from the pipe exit, it is fairly certain that the flow is not skewed in relation to the pipe center line. Since extreme care was exercised in alining the traversing mechanism, the reason for this asymmetry is not attributed to that source.

In figure 6 the distributions of u'/u are arranged to show their variation with Reynolds number at each of the three stations $\frac{x}{D} = 0, 2$, and 5. At $\frac{x}{D} = 0$, u'/u near the center line is constant with varying Reynolds number at a value of about 1.8 percent. Near the pipe wall the values range from 4 to 6 percent with no consistent variation with Reynolds number. At $\frac{x}{D} = 2$, u'/u near the center line varies from about 1.4 percent at $R = 21,300$ to about 2 percent at $R = 115,000$. The maximum values lie at about $r = 0.8$ inch and they vary from about 2.2 percent at the lowest Reynolds number up to 4.0 percent at the highest Reynolds number. At $\frac{x}{D} = 5$, u'/u near the center line varies from about 1.4 percent up to about 2.1 percent with increasing Reynolds number. The maximum values lie at about $r = \pm 0.7$ inch and vary from about 2 percent to 3.5 percent with increasing Reynolds number.

In figure 7 the distributions of v'/u are arranged to show their variation with Reynolds number at each of the three stations $\frac{x}{D} = 0, 2$, and 5. Near the center line v'/u is about 0.7 percent and no systematic variation with Reynolds number occurs at any station. In the mixing region downstream of the pipe walls v'/u is about 1.5 percent at all three stations, and at every station no systematic variation of v'/u with Reynolds number is observed.

In figure 8 distributions of u'/u are arranged to show the variation with x/D at each of the four Reynolds numbers. The same arrangement is presented for v'/u distributions in figure 9. Near the pipe center line no variation of either u'/u or v'/u is observed. The only changes occur in the mixing region formed by the wake of the pipe walls. In this region, the absolute values of u' decrease with increasing x/D whereas the absolute values of v' are essentially

constant. Thus, it appears that the turbulence tends to isotropy as x/D increases in the mixing region. Since u increases in this region as x/D increases, a decrease occurs in values of both u'/u and v'/u (figs. 6 and 7); and u'/u decreases more rapidly than v'/u .

CONCLUSIONS

A jet configuration consisting of a subsonic air jet issuing from a fully developed turbulent pipe flow and bounded by an annular jet in which the maximum velocity was maintained equal to the mean velocity across the inner pipe was investigated. From this investigation the following conclusions are drawn:

1. The turbulence in the jet was not isotropic. At the exit survey station the longitudinal turbulence intensity was about 2.5 times as great as the radial turbulence intensity at the jet center line and about 3 or 4 times as great near the inner pipe walls.
2. At the pipe exit, the ratio of the longitudinal turbulence velocity to the local mean velocity showed no systematic variation with Reynolds number. At stations 2 and 5 diameters from the exit, this ratio increased with increasing Reynolds number.
3. The ratio of radial turbulence velocity to local mean velocity showed no consistent variation with Reynolds number at any station.
4. Near the pipe center line both the longitudinal and radial turbulence intensities were constant from the pipe exit to a distance 5 diameters from the exit. In the mixing zone, the longitudinal turbulence intensity decreased more rapidly than the radial turbulence intensity with increasing distance from the exit, because the longitudinal turbulence velocity increased, whereas the radial turbulence velocity was essentially constant. The most rapid decrease in longitudinal turbulence velocity occurred between the exit station and the station 2 diameters from the exit.

Langley Aeronautical Laboratory
National Advisory Committee for Aeronautics
Langley Field, Va., January 24, 1951

REFERENCES

1. Schubauer, G. B., and Klebanoff, P. S.: Theory and Application of Hot-Wire Instruments in the Investigation of Turbulent Boundary Layers. NACA ACR 5K27, 1946.
2. Prandtl, L.: The Mechanics of Viscous Fluids. The Laws of Surface Friction from Experiments on Flows in Tubes. Resistance Formulas. Effect of Roughness. Vol. III of Aerodynamic Theory, div. G, sec. 22, W. F. Durand, ed., Julius Springer (Berlin), 1935, pp. 135-145.

TABLE I.- TURBULENT FLUCTUATION VELOCITIES

[All velocities in feet per second]

R r (in.)	21,300		45,000		84,000		115,000	
	u'	v'	u'	v'	u'	v'	u'	v'
$\frac{x}{D} = 0$								
1.2	0.08	0.07	0.18	0.17	0.46	0.36	0.58	0.54
1.1	.27	.06	.33	.12	.62	.32	.79	.46
1.05	.25	.04	1.10	.15	2.10	.40	2.27	.67
.975	.69	.09	1.52	.27	2.52	.46	3.01	.76
.95	.63	.12	1.35	.26	2.47	.37	3.27	.73
.9	.51	.13	1.37	.29	2.70	.49	3.60	.84
.8	.49	.13	1.39	.32	2.86	.67	3.69	.94
.7	.51	.13	1.31	.35	2.78	.56	3.70	.98
.6	.50	.14	1.23	.34	2.70	.58	3.46	.99
.4	.45	.13	1.10	.29	2.23	.55	2.93	.99
.2	.34	.12	.93	.28	1.73	.55	2.35	.97
.1	.30	.12	.72	.27	1.63	.53	2.07	.96
0	.29	.13	.69	.29	1.42	.55	1.82	.95
-.1	.30	.13	.66	.31	1.37	.55	1.77	.95
-.2	.33	.14	.79	.31	1.51	.57	1.95	1.00
-.4	.44	.15	1.01	.36	1.98	.64	2.46	1.12
-.6	.48	.16	1.18	.38	2.37	.77	2.87	1.21
-.7	.48	.16	1.30	.39	2.56	.82	3.25	1.26
-.8	.56	.15	1.37	.39	2.62	.77	3.42	1.25
-.9	.59	.14	1.35	.34	2.64	.76	3.43	1.05
-.95	.59	.13	1.32	.30	2.41	.67	3.15	.98
-.975	.56	.11	1.44	.29	2.33	.70	3.05	.98
-.105	.86	.04	1.50	.16	2.41	.34	4.49	.52
-.11	.30	.05	.33	.14	1.16	.19	.76	.31
-.12	.08	.06	.20	.20	.47	.29	.49	.55
$\frac{x}{D} = 2$								
1.2	0.10	0.08	0.25	0.19	0.62	0.36	1.04	0.54
1.1	.14	.10	.42	.23	1.07	.44	1.78	.69
1.0	.15	.11	.56	.26	1.18	.49	1.97	.77
.95	.24	.13	.66	.29	1.50	.50	2.30	.79
.9	.27	.13	.79	.31	1.84	.52	2.91	.85
.8	.34	.14	.96	.34	2.19	.55	4.37	.92
.7	.38	.15	1.04	.34	2.35	.56	4.50	.94
.6	.37	.14	1.01	.34	2.21	.57	3.75	.96
.4	.32	.14	.92	.31	2.07	.57	3.22	.94
.2	.29	.13	.87	.27	1.80	.55	2.79	.96
.1	.30	.13	.76	.27	1.58	.53	2.58	.97
0	.26	.13	.73	.27	1.55	.53	2.38	.96
-.1	.29	.13	.71	.27	1.79	.55	2.22	.96
-.2	.28	.14	.73	.30	1.83	.56	2.31	.98
-.4	.32	.16	.90	.38	2.38	.64	2.70	1.07
-.6	.35	.17	1.00	.39	2.88	.74	3.40	1.18
-.7	.37	.17	1.03	.38	3.06	.80	3.65	1.26
-.8	.35	.18	.99	.39	2.84	.76	3.80	1.21
-.9	.29	.15	.81	.34	2.73	.63	2.98	.96
-.95	.30	.14	.68	.29	2.33	.53	2.32	.80
-.105	.23	.13	.56	.27	1.89	.43	1.88	.66
-.11	.14	.09	.31	.24	1.39	.32	1.62	.53
-.12	.09	.07	.18	.25	.93	.32	.74	.56
$\frac{x}{D} = 5$								
1.2	0.15	0.08	0.40	0.15	1.02	0.44	1.87	0.73
1.1	.18	.08	.45	.27	1.13	.45	2.09	.75
1.0	.21	.09	.54	.27	1.36	.47	2.13	.76
.9	.26	.10	.64	.28	1.76	.47	2.29	.80
.8	.31	.11	.76	.29	1.98	.49	2.89	.82
.7	.32	.13	.81	.32	2.27	.52	3.42	.86
.6	.37	.14	.86	.31	2.31	.55	3.47	.90
.4	.35	.15	.85	.30	2.22	.53	3.51	.87
.2	.30	.14	.73	.26	1.88	.52	3.03	.86
.1	.27	.14	.67	.27	1.57	.53	2.77	.86
0	.26	.15	.63	.28	1.38	.53	2.67	.85
-.1	.27	.15	.62	.27	1.29	.55	2.49	.89
-.2	.27	.15	.71	.29	1.28	.57	2.43	.92
-.4	.32	.17	.83	.35	1.94	.67	2.85	1.03
-.6	.36	.15	.86	.41	2.28	.73	3.38	1.12
-.7	.33	.15	.83	.40	2.18	.73	3.46	1.16
-.8	.32	.13	.79	.37	2.19	.66	3.26	1.00
-.9	.29	.13	.68	.34	1.85	.56	2.72	.88
-.10	.27	.10	.57	.32	1.53	.47	2.09	.72
-.11	.21	.09	.42	.29	1.19	.40	1.83	.68
-.12	.16	.08	.37	.29	.95	.37	1.54	.67

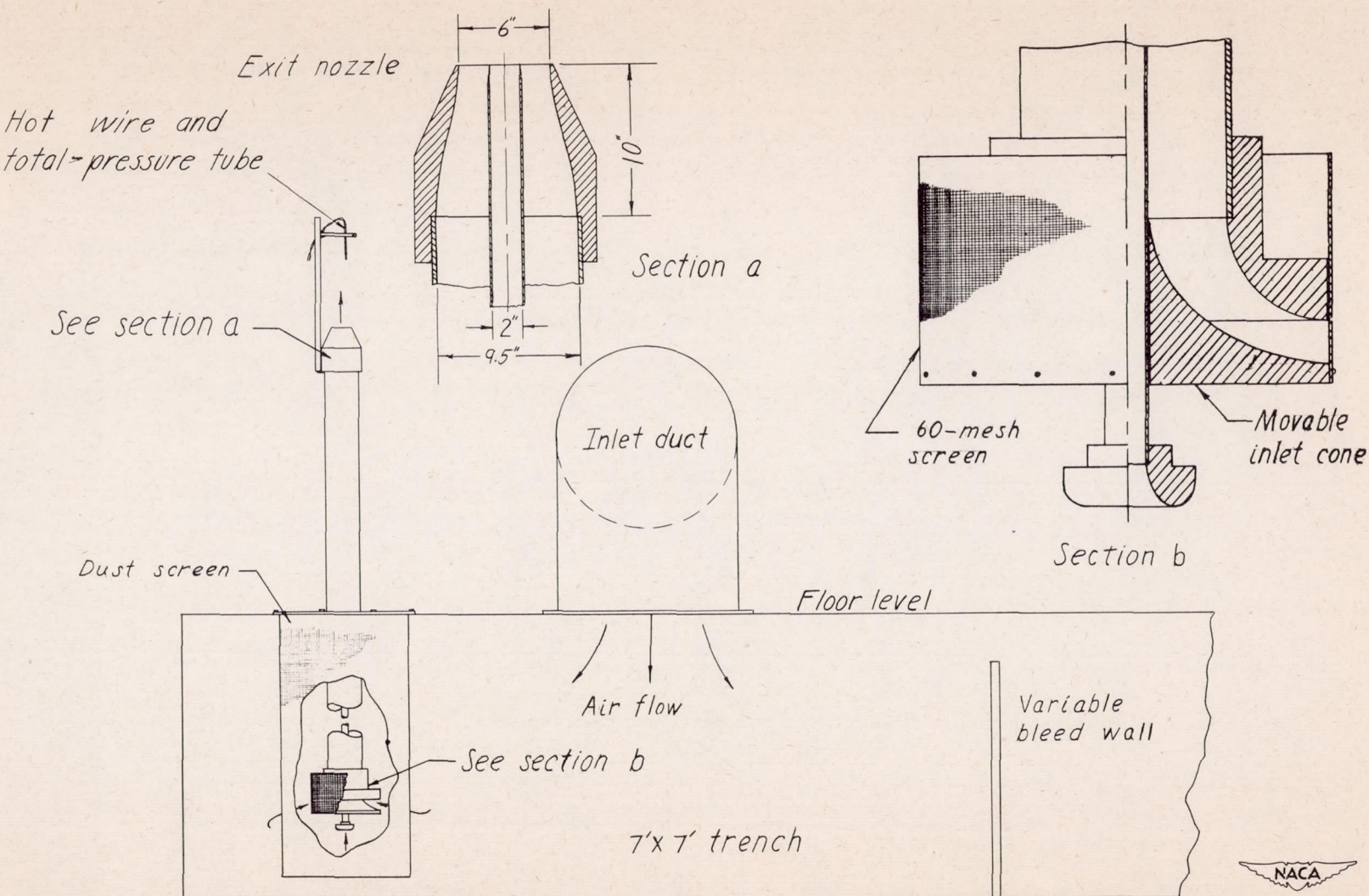
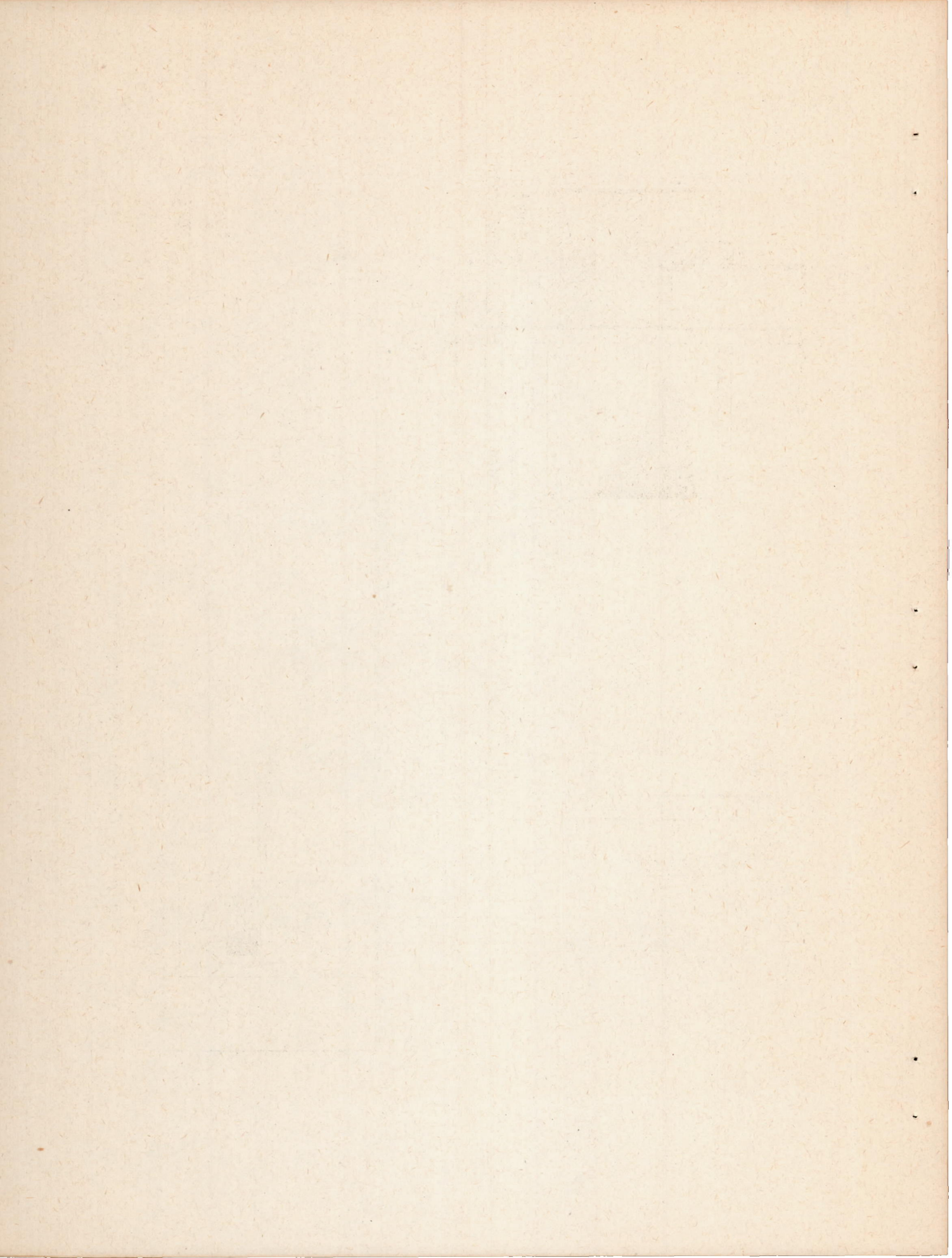


Figure 1.- General arrangement of test apparatus.



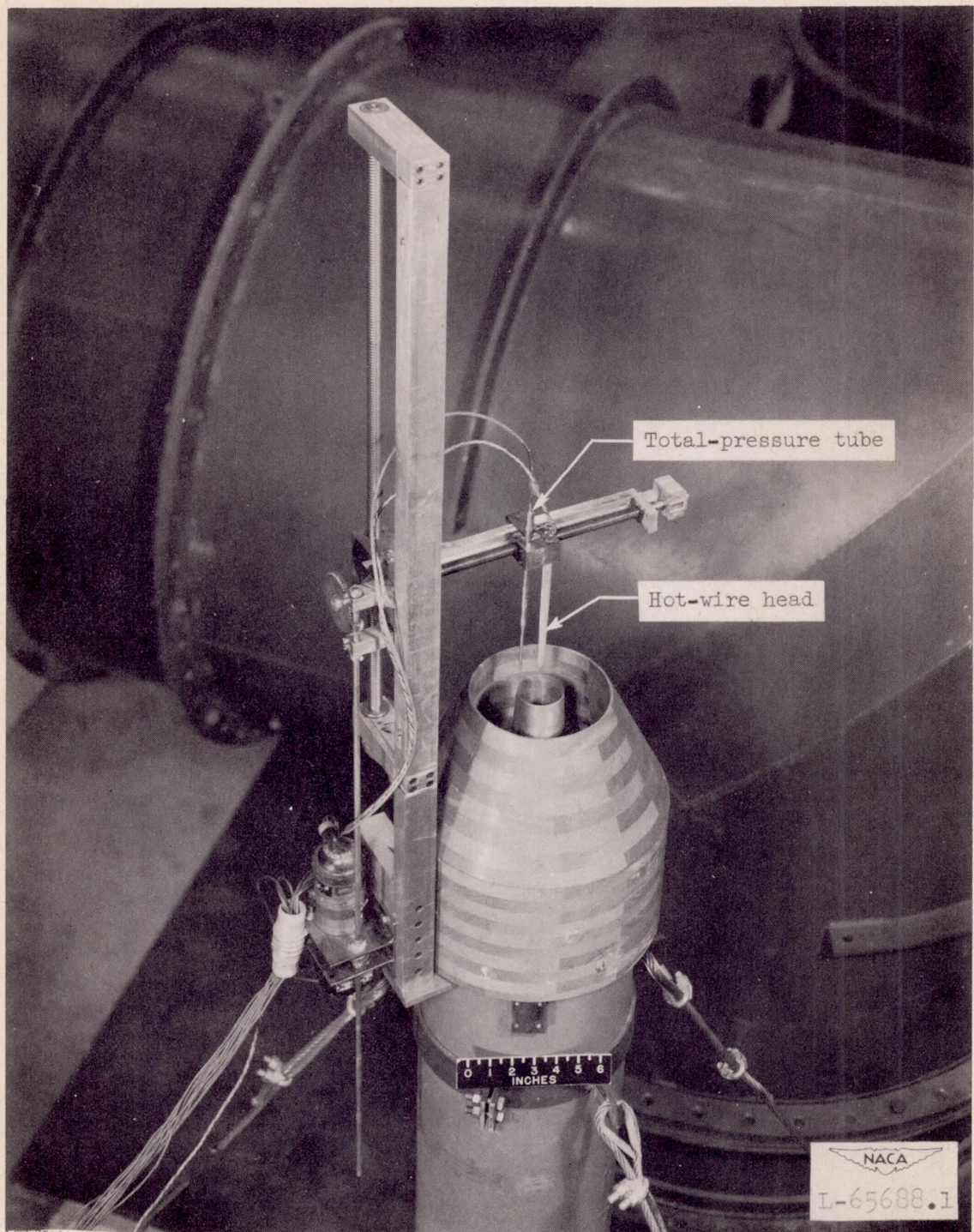
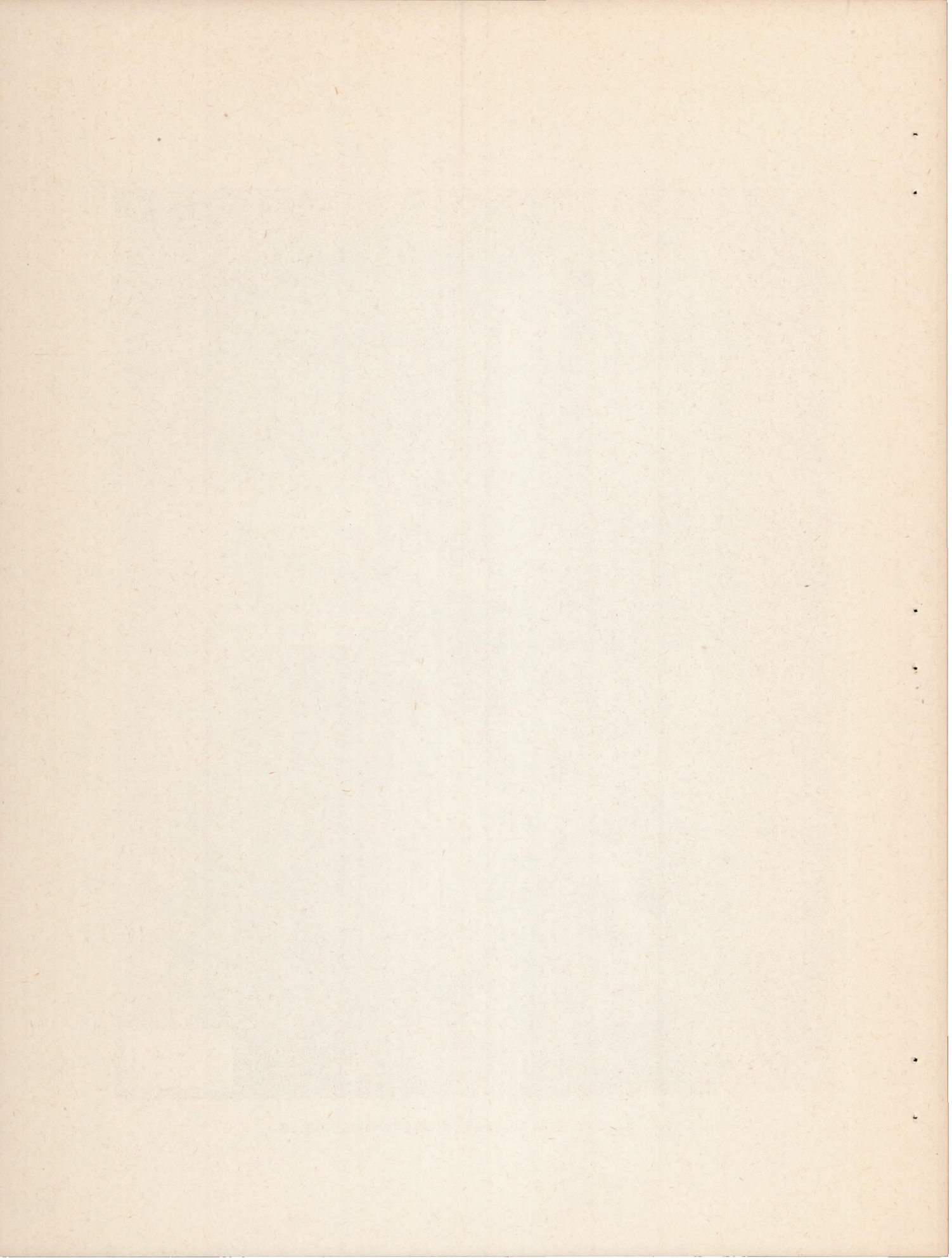


Figure 2.- Hot-wire drive mechanism.



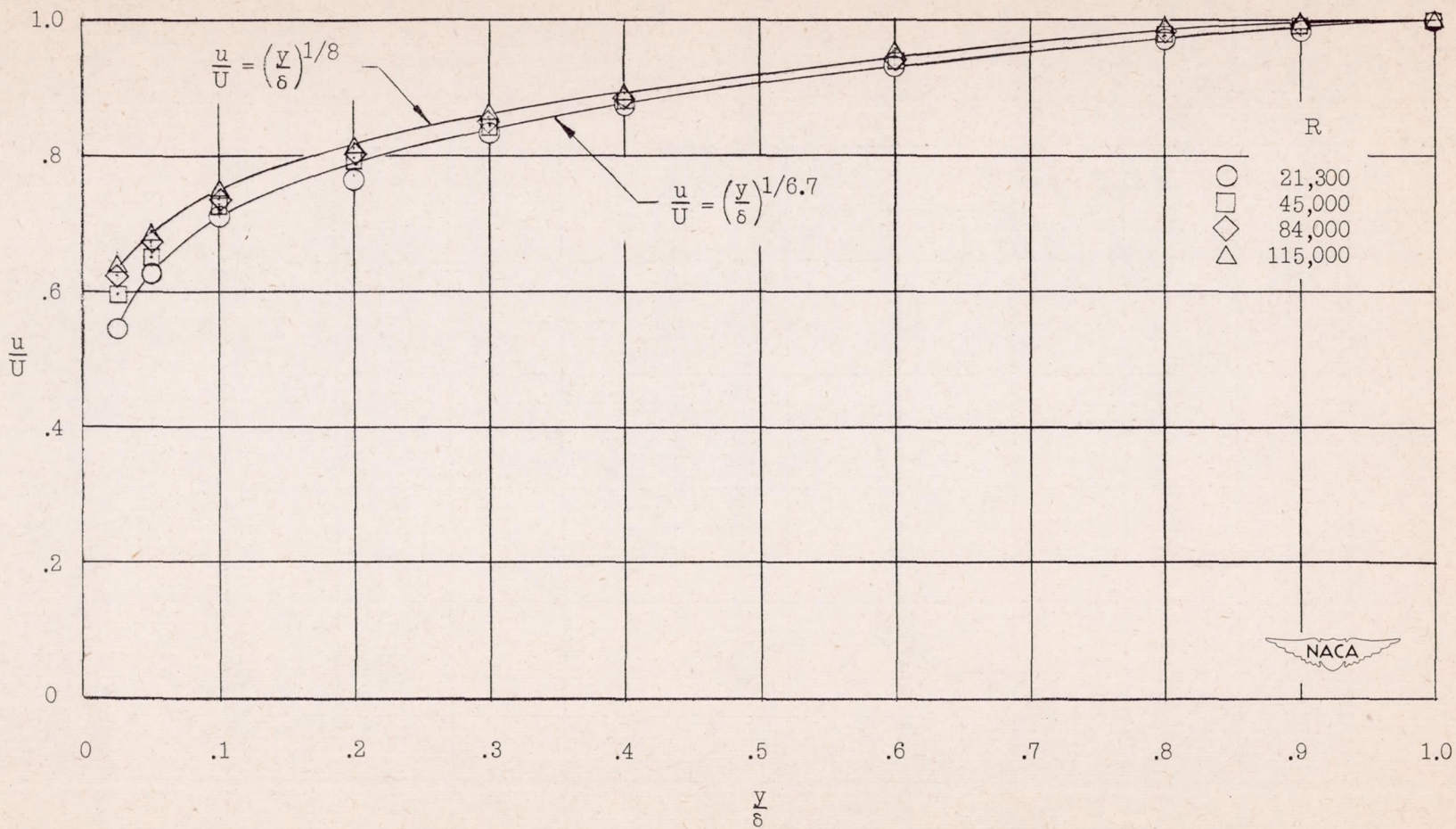


Figure 3.- Mean-velocity distributions at pipe exit.

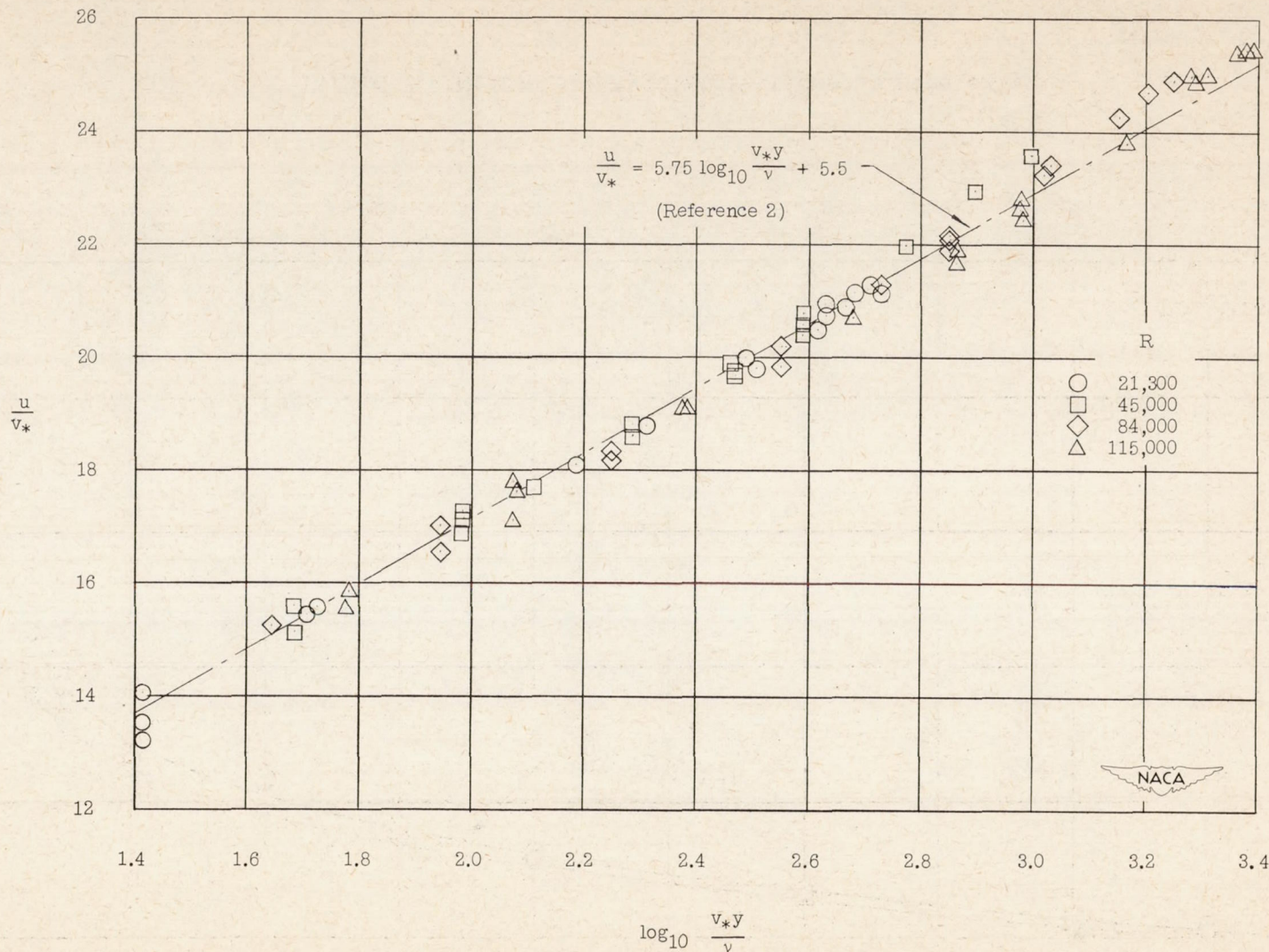


Figure 4.- Comparison of velocity distributions with the universal distribution law.

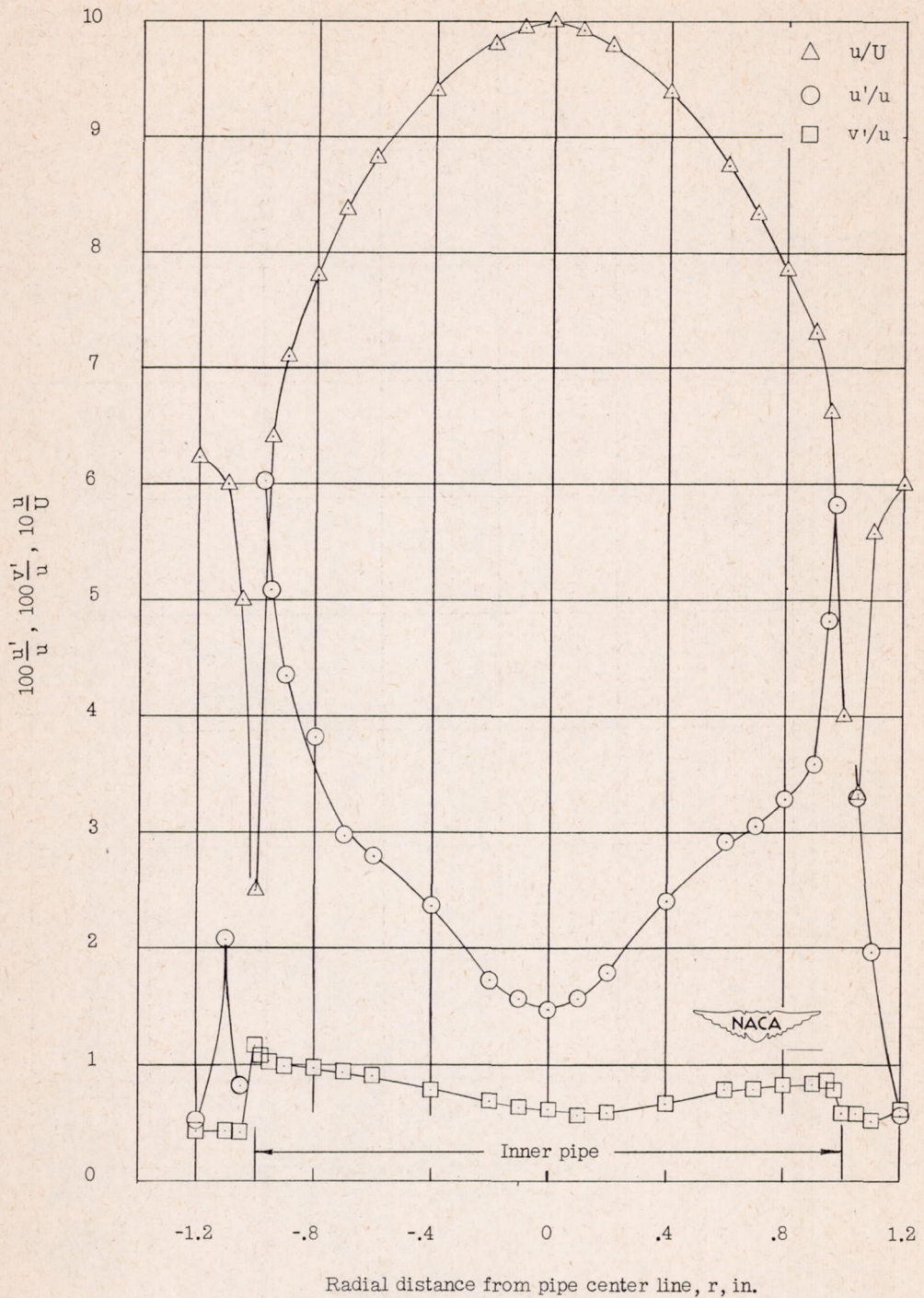
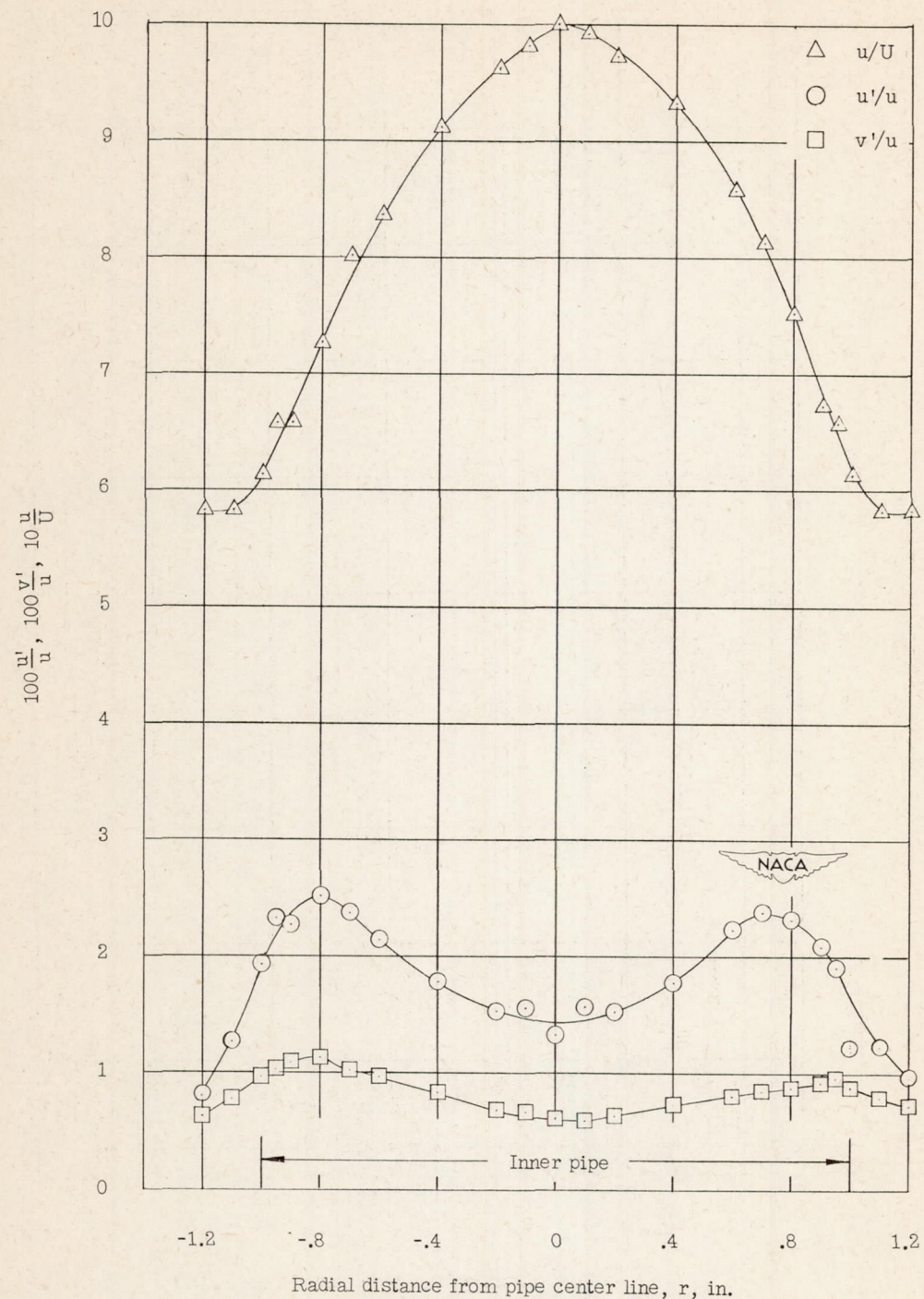
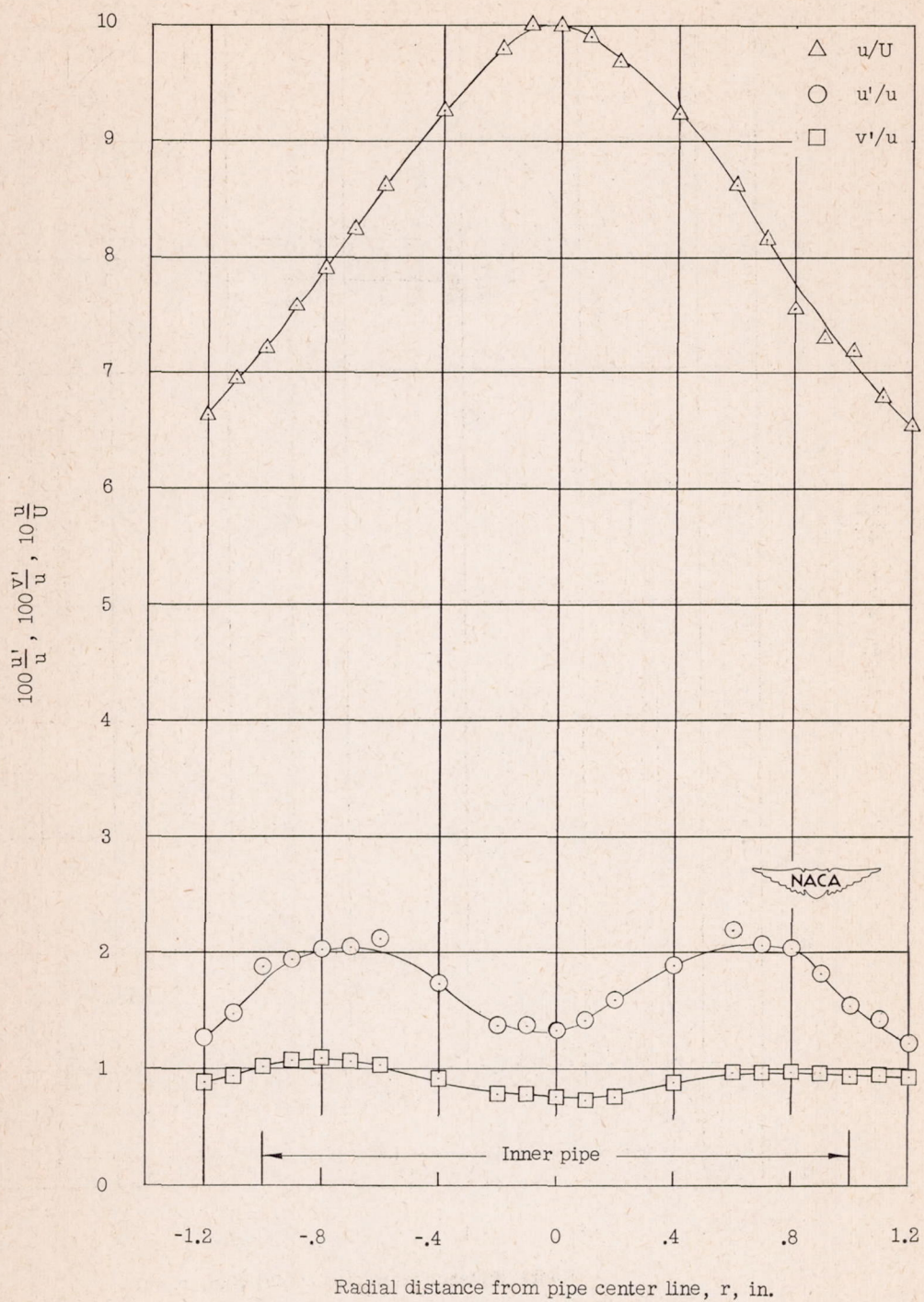
(a) $R = 21,300$; $\frac{X}{D} = 0$.

Figure 5.- Turbulence intensity and velocity distributions.



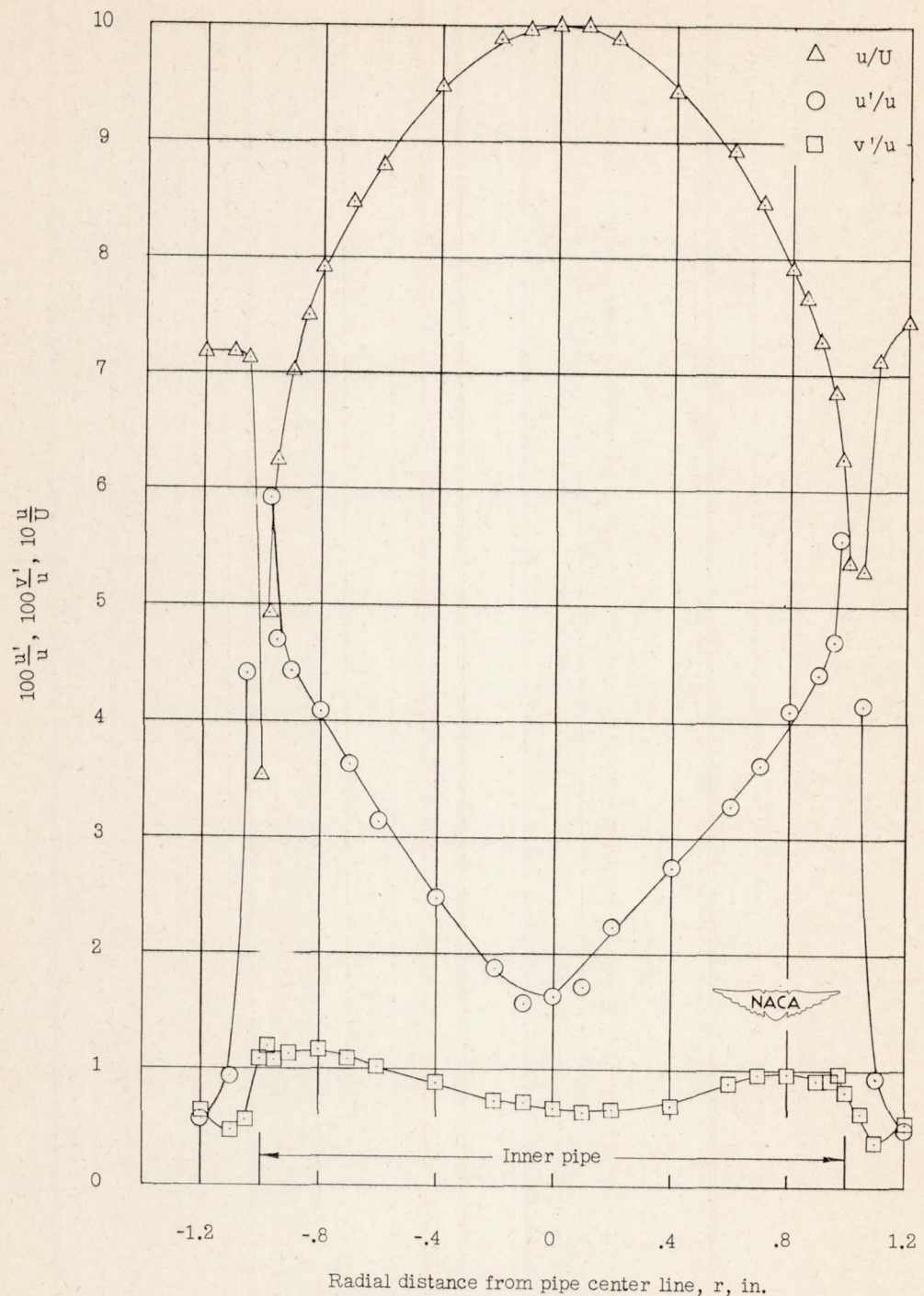
(b) $R = 21,300$; $\frac{X}{D} = 2$.

Figure 5.- Continued.



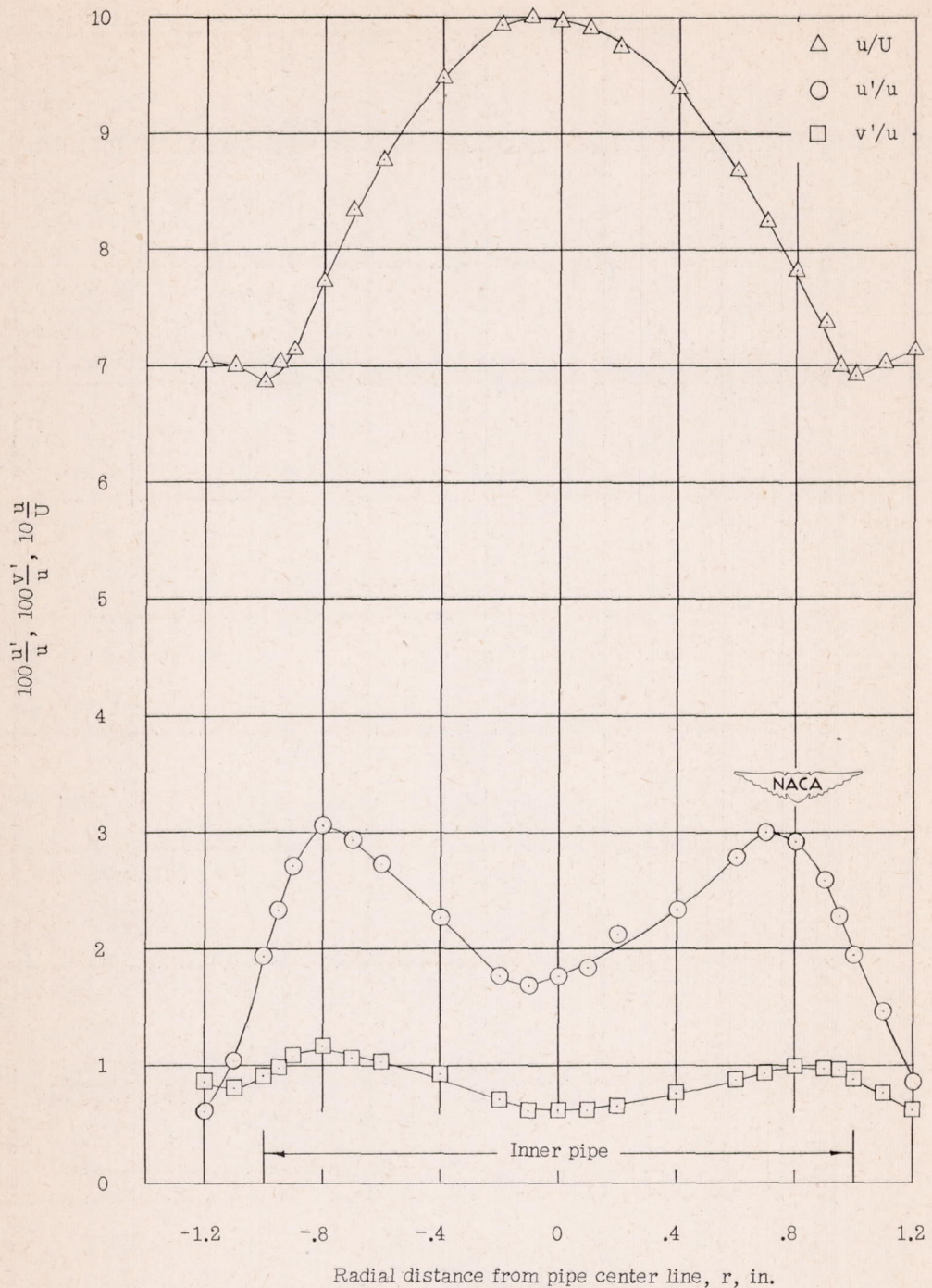
(c) $R = 21,300$; $\frac{X}{D} = 5$.

Figure 5.- Continued.



(d) $R = 45,000$; $\frac{X}{D} = 0$.

Figure 5.- Continued.



(e) $R = 45,000$; $\frac{X}{D} = 2$.

Figure 5.- Continued.

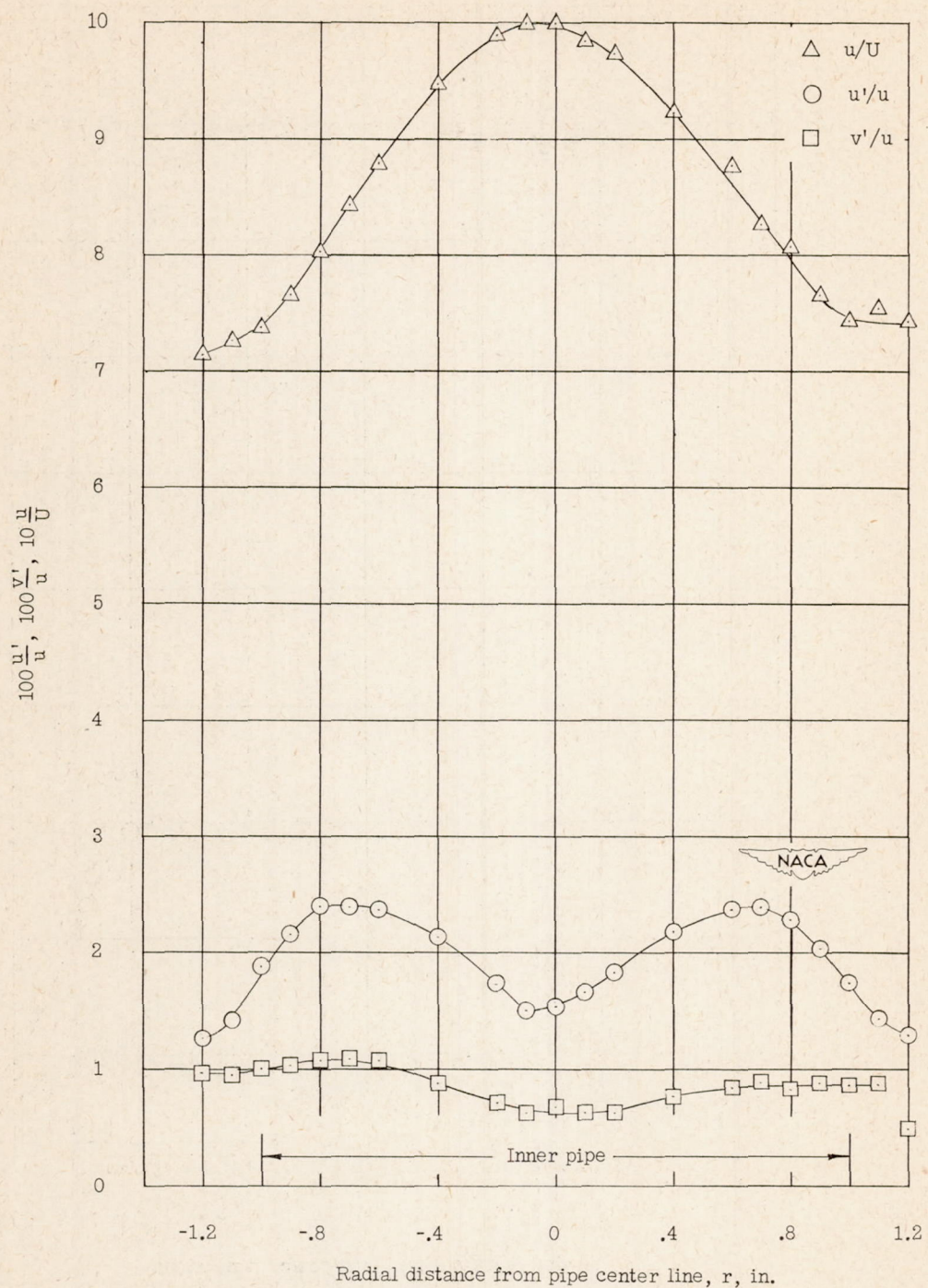


Figure 5.- Continued.

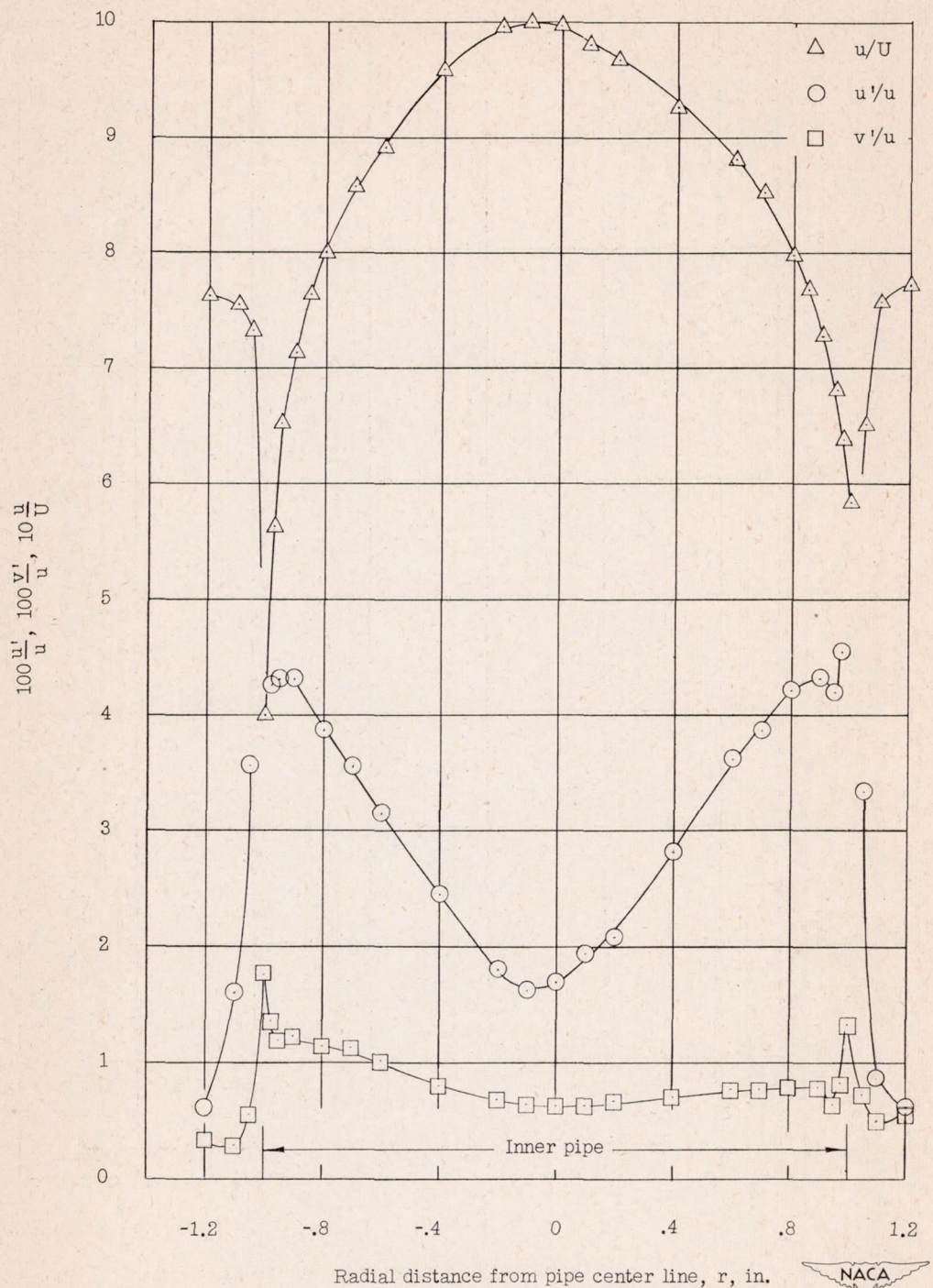
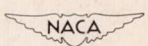
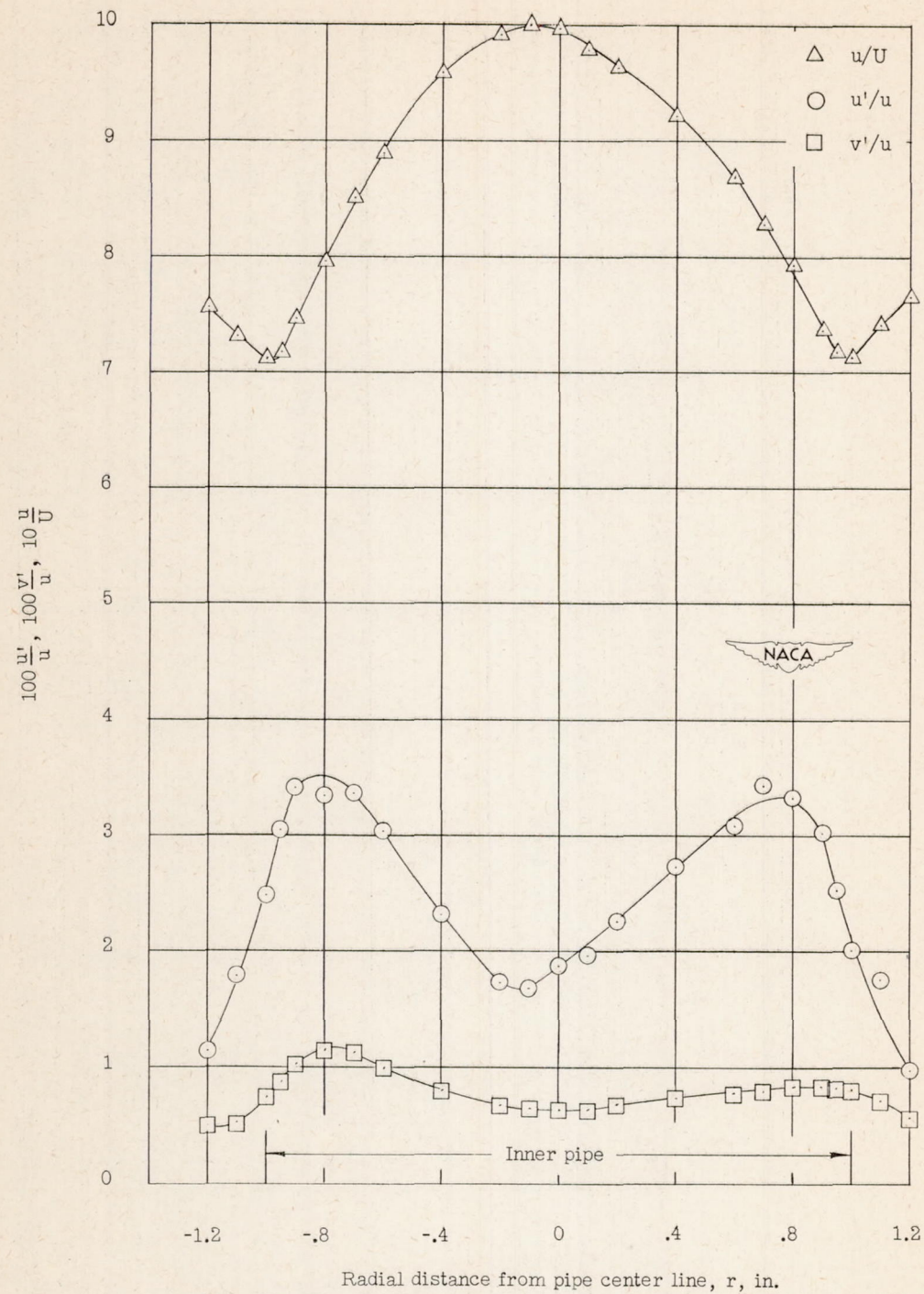
(g) $R = 84,000$; $\frac{x}{D} = 0$.

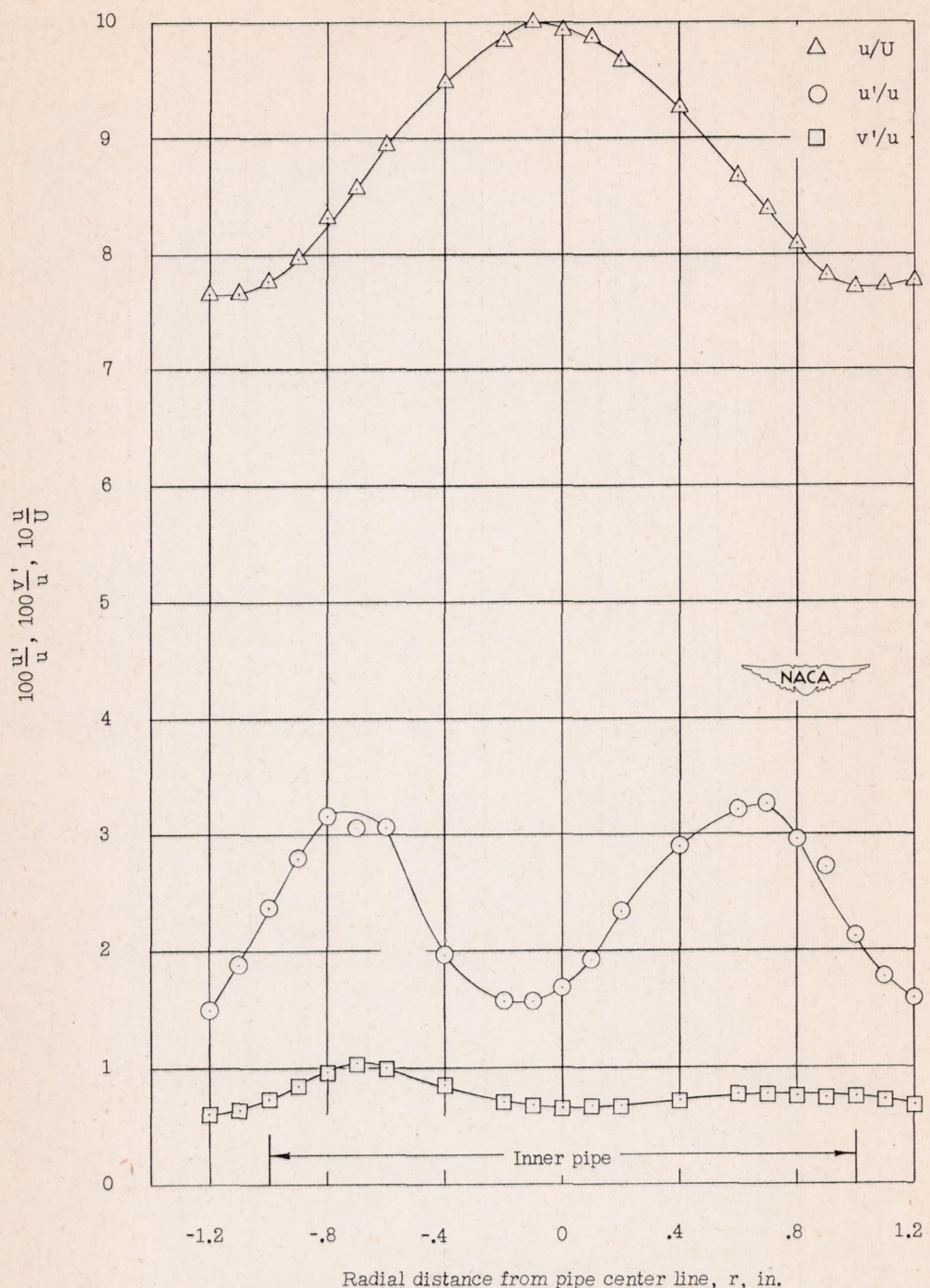
Figure 5.- Continued.





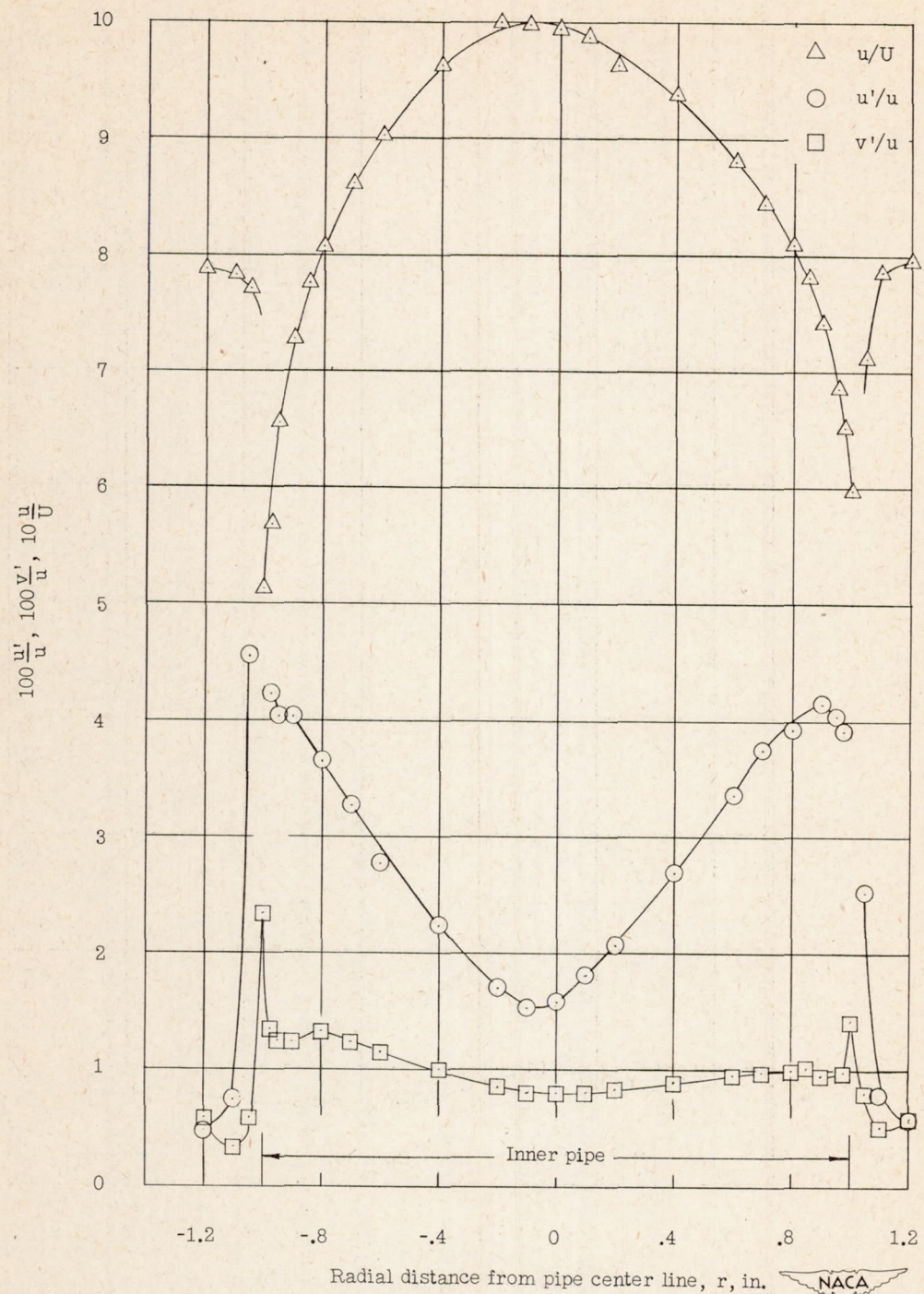
(h) $R = 84,000$; $\frac{X}{D} = 2$

Figure 5.- Continued.



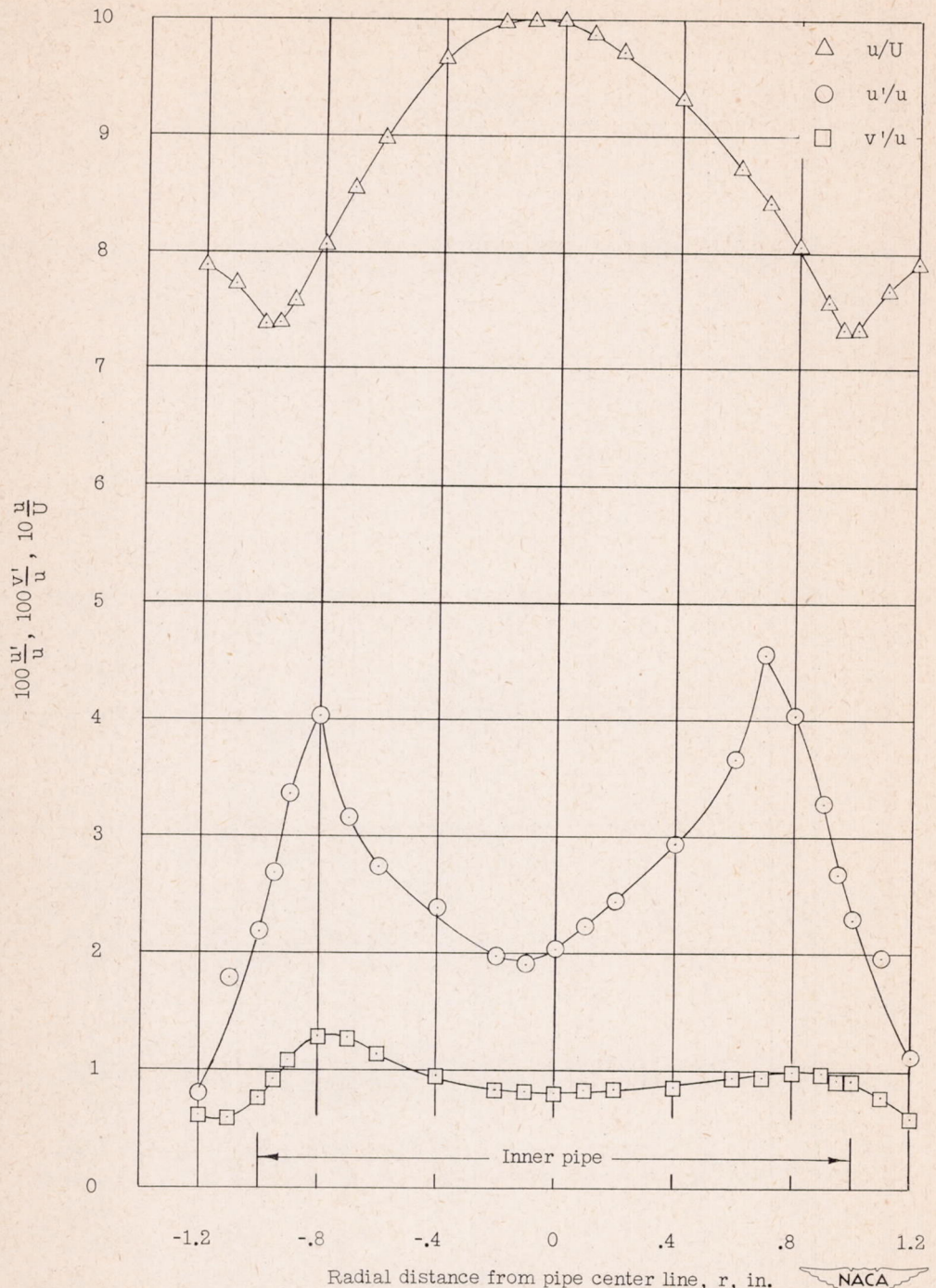
(i) $R = 84,000$; $\frac{X}{D} = 5$.

Figure 5.- Continued.



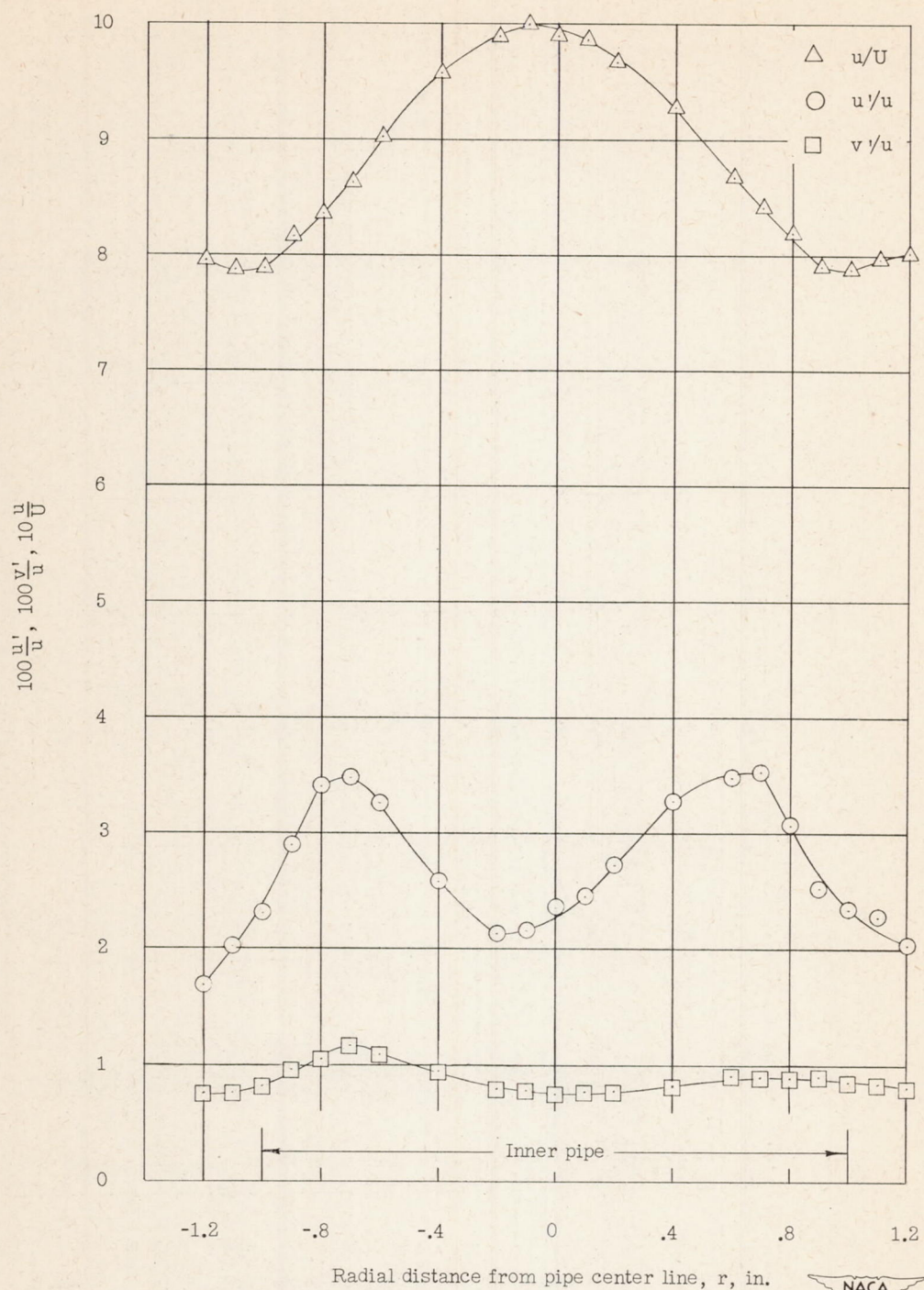
(j) $R = 115,000$; $\frac{x}{D} = 0$.

Figure 5.- Continued.



(k) $R = 115,000$; $\frac{X}{D} = 2$.

Figure 5.- Continued.



(1) $R = 115,000$; $\frac{X}{D} = 5$.

Figure 5.- Concluded.

NACA

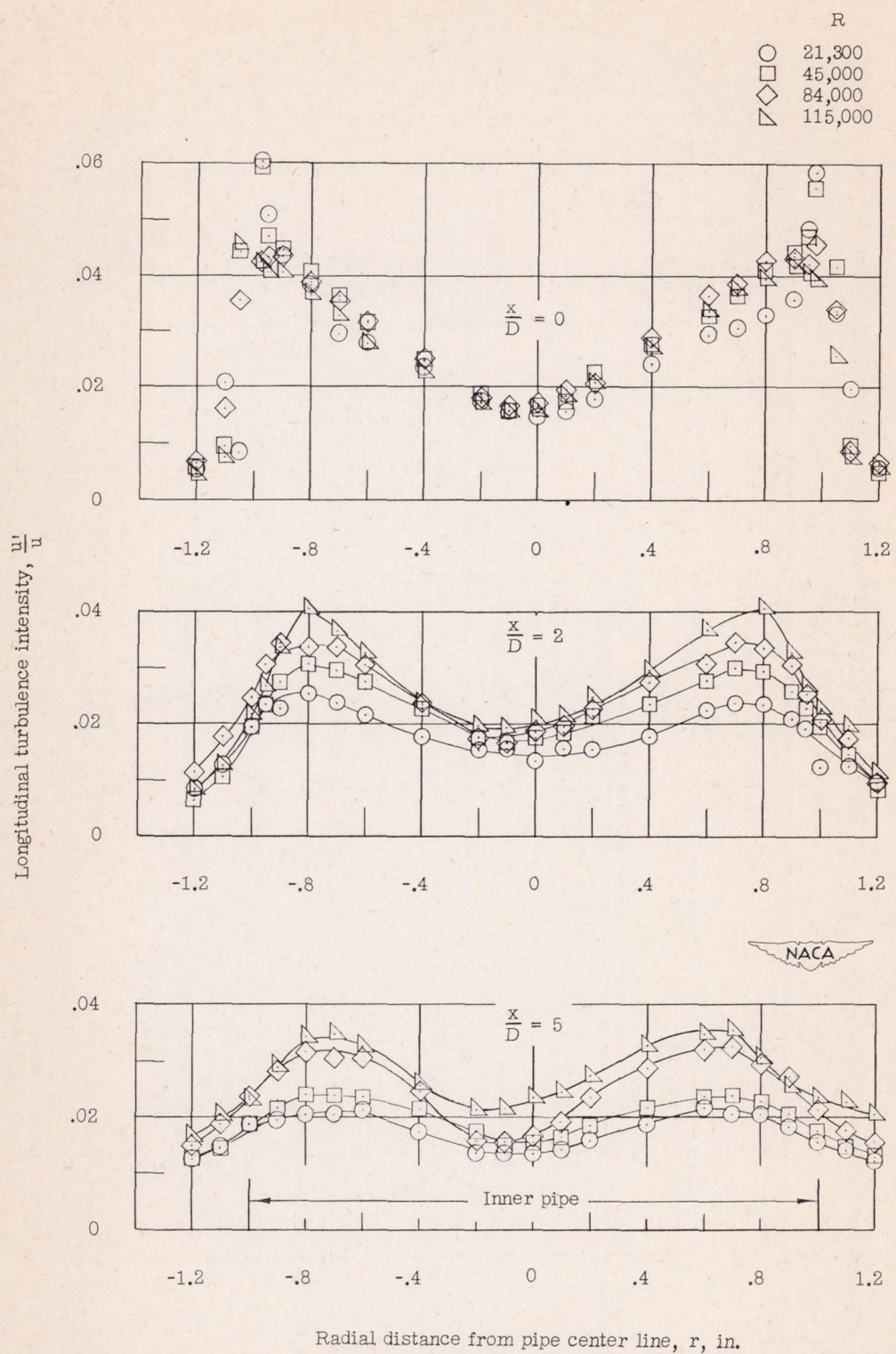


Figure 6.- Variation of longitudinal turbulence intensity with Reynolds number.

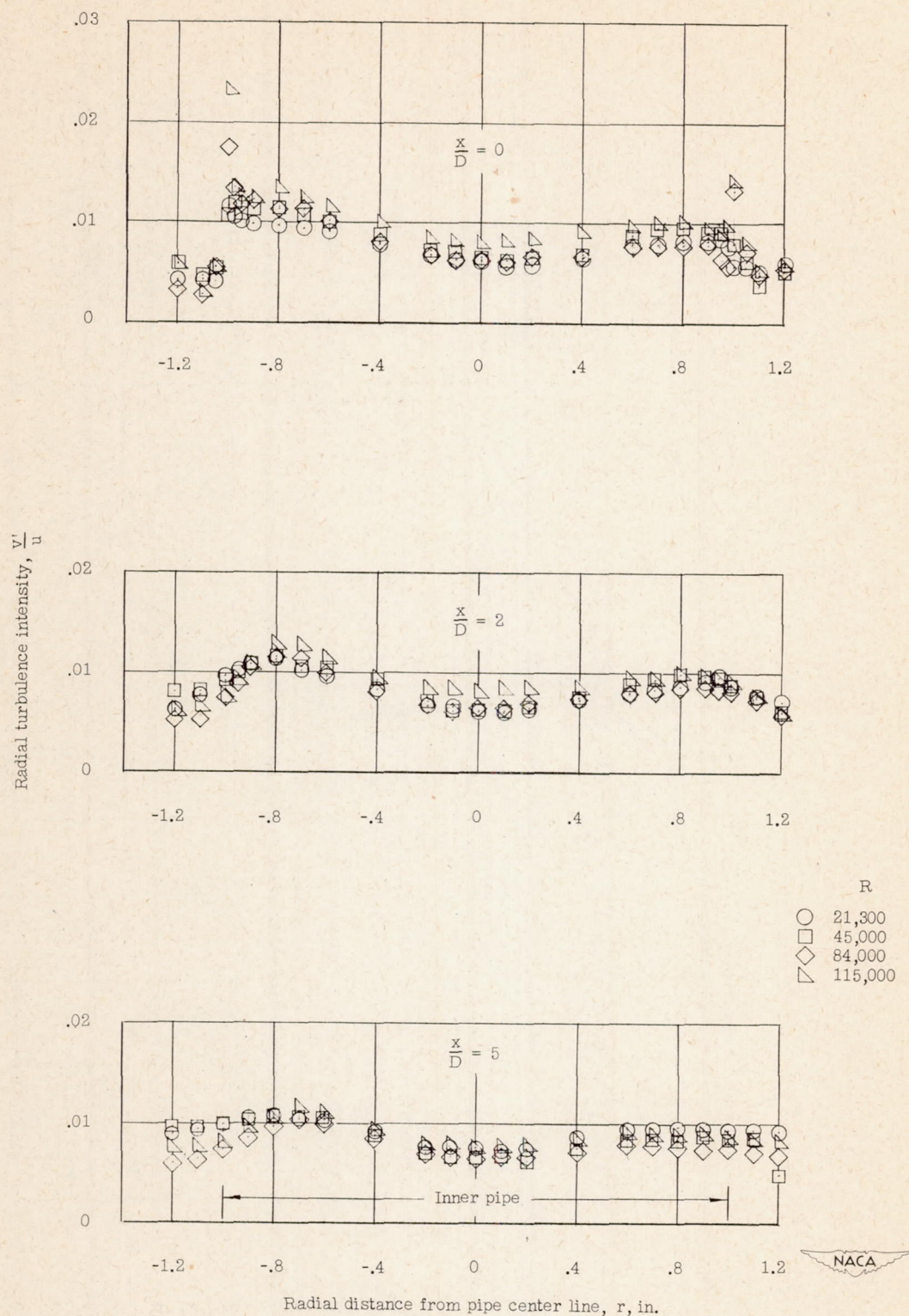


Figure 7.- Variation of radial turbulence intensity with Reynolds number.

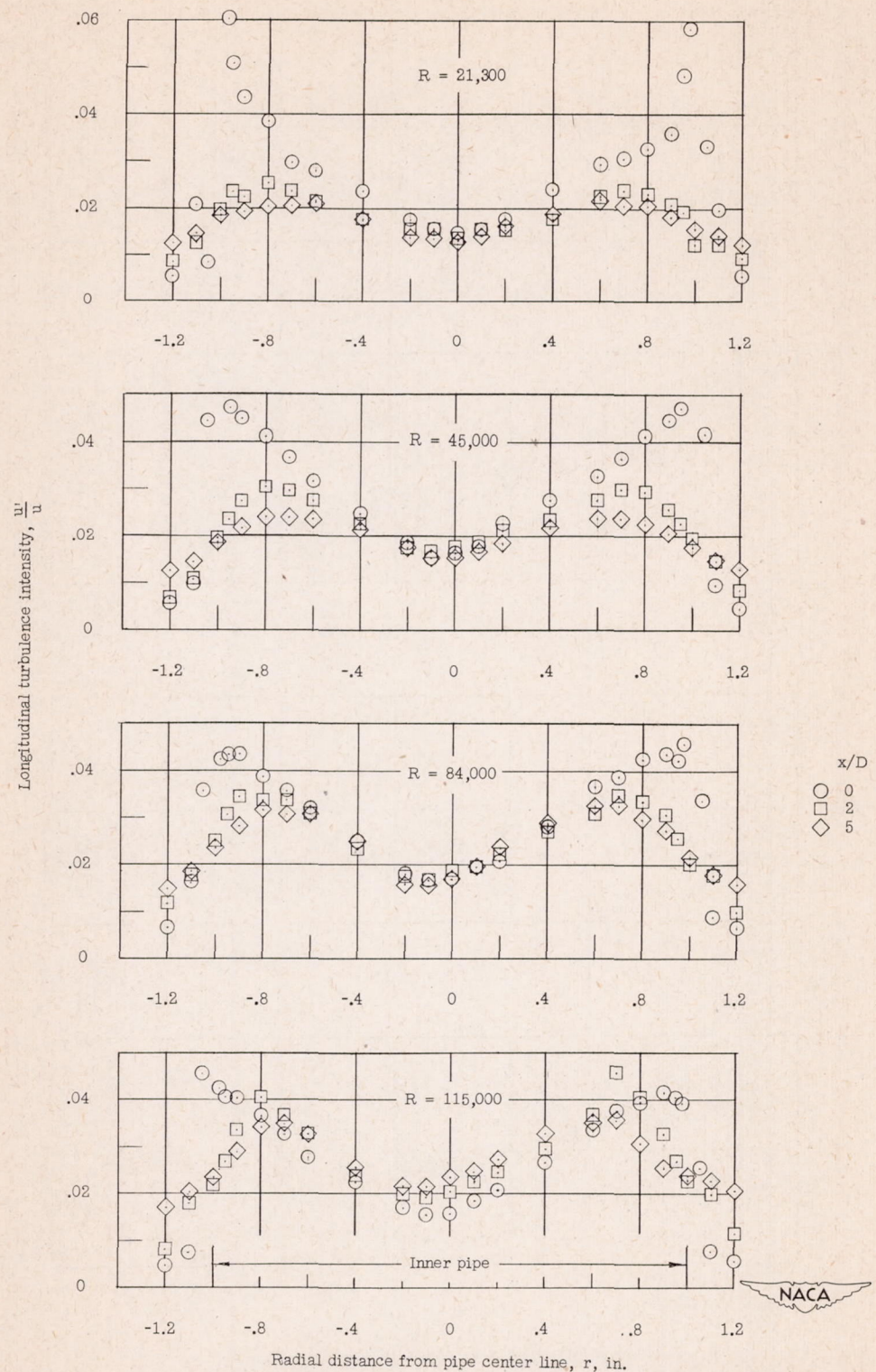
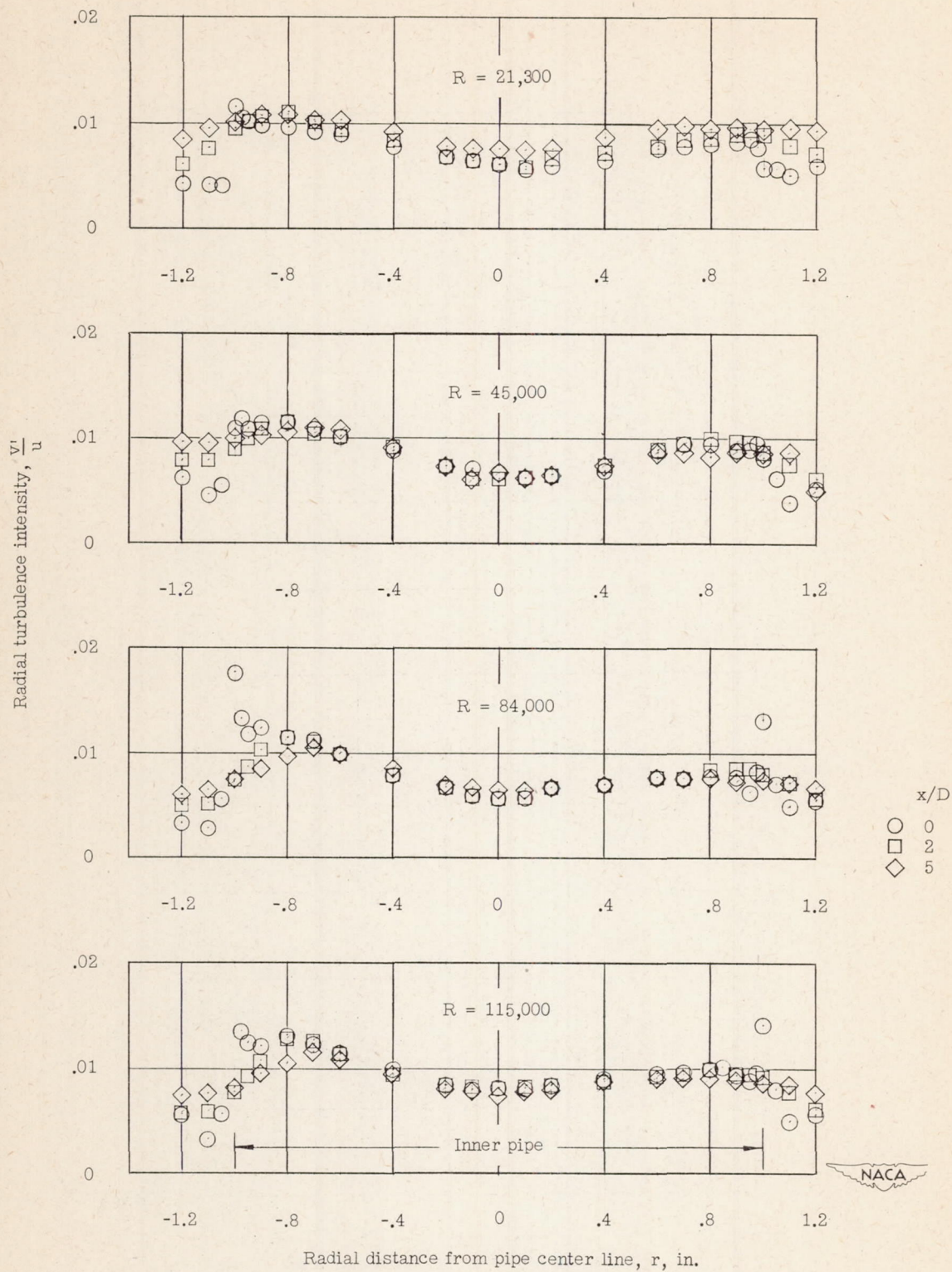


Figure 8.- Variation of longitudinal turbulence intensity with x/D .

Figure 9.- Variation of radial turbulence intensity with x/D .